Desalination and Water Treatment
www.deswater.com
doi: 10.1080/19443994.2014.928910

55 (2015) 1372–1379
July

Taylor & Francis
Taylor & Francis Group

Fixed-bed column studies for the removal of cationic and anionic dyes by chemically modified oil palm empty fruit bunch fibers: single- and multi-solute systems

Mohd Shaiful Sajab[a], Chin Hua Chia[a,*], Sarani Zakaria[a], Mika Sillanpää[b]

[a]*Materials Science Programme, Faculty of Science and Technology, School of Applied Physics, Universiti Kebangsaan Malaysia, 43600 Bangi, Selangor, Malaysia, Tel. +60177872657; email: mohdshaifulsajab@yahoo.com (M.S. Sajab), Tel. +603 8921 5473; Fax: +603 8921 3777; email: chiachinhua@yahoo.com (C.H. Chia), Tel. +603 8921 3261; email: sarani_zakaria@yahoo.com (S. Zakaria)*
[b]*Faculty of Technology, Lappeenranta University of Technology, Patteristonkatu 1, FI-50100 Mikkeli, Finland, Tel. +358 400 205 215; email: Mika.Sillanpaa@lut.fi*

Received 7 November 2013; Accepted 9 May 2014

ABSTRACT

The adsorption performance of cationically and anionically modified oil palm empty fruit bunch fibers toward methylene blue (MB) and phenol red (PR) was investigated using single- and multi-solute systems in a fixed-bed system. The experimental data were fit with Thomas and Clark column adsorption models to evaluate different experimental conditions (adsorbate dose, bed height, column temperature, and flow rate). The results suggest that the adsorption mechanism was that of monolayer and heterogeneous. The service time of each bed was estimated using a bed depth service time model by considering the adsorption rate. The regeneration of the adsorbent for up to five adsorption/desorption cycles was investigated, suggesting the excellent reusability of the adsorbent column. The simultaneous removal of mixed MB and PR was achieved using both fibers packed with different configurations.

Keywords: Adsorption; Clark; Fixed-bed; Natural adsorbent; Thomas

1. Introduction

The management of industrial dye effluent is becoming a challenging task due to the rapid growth in the consumption of dyes every year [1]. The discharge of dyes into the waste stream could have an impact on the aquatic ecosystem. Therefore, strict regulations are introduced to control and monitor the quality of discharge water from various industries [2].

The development of different techniques for the treatment of dye effluent using physical, chemical, and biological means has been conducted since many years. Adsorption has been proven to be one of the promising approaches for the removal of dye compounds from aqueous solution due to its effectiveness, flexibility, simplicity of design, and ease of operation [1,3]. In addition, many efforts have also focused on adsorbing multi-component dyes that are representative of real industrial waste effluent, such as mixtures of dyes, organic compounds, and heavy metals [2,4–6].

Currently, numerous proposals have expanded the idea of utilizing inexpensive adsorbents from natural materials, such as agricultural wastes and minerals for the removal of dyes [7]. Besides, various chemical

*Corresponding author.

treatments have been proposed to enhance the adsorption efficiency of agricultural wastes [8].

Malaysia is the second largest palm oil producer in the world [9]. Large quantity of empty fruit bunch (EFB) fibers is generated from palm oil industries and is used as fertilizer, composite making, etc. [10,11]. Previous study on the removal of methylene blue (MB) and phenol red (PR) using EFB fibers revealed the potential application of EFB fibers for the treatment of dye effluent [12]. In this work, the cationically and anionically modified EFB fibers were packed in column and used for the removal of MB and PR using a fixed-bed adsorption system. The effects of various parameters, including pH, dyes concentration, temperatures, and bed height, on the adsorption performance of the EFB fibers were investigated. The regeneration performance of both fibres was investigated for five adsorption/desorption cycles. In addition, simultaneous adsorption of MB and PR from a mixed dyes solution to a column containing both modified EFB fibers was carried out. The effect of configurations of both fibers in the packed column on the performance of dye removal was investigated.

2. Experimental

2.1. Preparation of chemically modified EFB fibers

Oil palm EFB fibers were purchased from Szetech Engineering Sdn. Bhd. (Malaysia) and chemically modified according to a previously described procedure [12]. The fibers were firstly pre-treated with NaOH and were then subjected to citric acid (CA) and polyethylenimine (PEI) chemical modification. Briefly, both treatments were performed at an EFB fiber concentration of 100 g/L using either a solution of 0.6 M CA or 5% PEI (w/v) (M_W ~750,000, 50 wt.% in H_2O). The CA-EFB fibers were transformed using an esterification process by heating to 120˚C, whereas the PEI-EFB fibers were treated with glutaraldehyde (1% v/v). The modified EFB fibers were washed several times to completely remove excess chemicals. The resulting fibers were dried and stored in a desiccator until further use.

2.2. Preparation of dye solutions

MB trihydrate (Mallinckrodt $C_{16}H_{18}N_3SCl$, ≥99%) and PR ($C_{19}H_{14}O_5S$, Sigma–Aldrich) solutions were prepared from stock solutions. The concentrations of the MB and PR were measured using a UV–vis spectrophotometer at a λ_{max} of 665 and 430 nm, respectively. MB and PR solutions were prepared at different concentrations to afford absorbance values ranging from 0.1 to 1. The spectroscopic data were used to generate a standard calibration curve. The pH of the MB and PR solutions was adjusted using NaOH and HCl solutions. The calibration curves for mixtures of MB and PR dyes at different ratio (Fig. 1) indicate that there were no chemical interactions between the two dye molecules, in which each dye still projected its own absorbance band.

2.3. Column adsorption

Continuous dye adsorption experiments were performed using a fixed-bed column equipped with a water jacket (with an internal diameter of 3 cm and a length of 30 cm) (see Fig. 2). The CA-EFB and PEI-EFB fibers were packed in the column, and the dye solution was pumped through the column at different influent flow rates (5, 10 and 15 mL/min), which was controlled by a rotameter. The pH of the MB and PR effluent was set to pH 7 and 3, respectively, as discussed in previous study [12]. The concentration of dye was varied from 200 to 400 mg/L. The temperature of the fixed-bed column (20, 40, and 60˚C) was maintained during the course of the study using water jacket connected to a water bath circulator. The concentration of dye in the effluent was measured as a function of time until the breakthrough of the fixed-bed column was achieved.

2.4. Desorption and regeneration studies

The adsorption of MB and PR (300 mg/L) was evaluated using a fixed-bed CA-EFB and PEI-EFB column until the breakthrough was achieved. Subsequently, the desorbing solvent HCl (0.1 M) was pumped into the fixed-bed column packed with

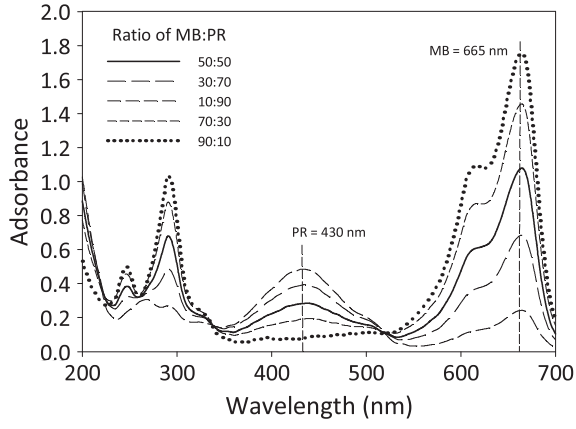

Fig. 1. Calibration of mixed dyes (MB and PR) at different concentration ratios.

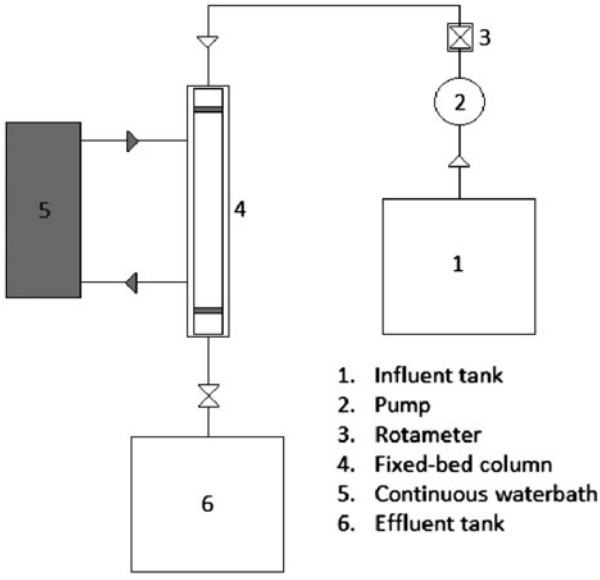

Fig. 2. Schematic diagram of the fixed-bed adsorption system.

adsorbed dyes until the amount of dye desorbed was nearly zero. The concentration of the desorbed dyes was calculated using the following equation:

$$\text{Amount of dye desorbed } (\%) = \frac{\text{Concentration desorbed (mg/L)}}{\text{Concentration adsorbed (mg/L)}} \times 100 \quad (1)$$

The packed fibers were washed with deionized water to remove the desorbing solvent. Regeneration studies were performed using five adsorption/desorption cycles.

2.5. Simultaneous adsorption of mixed dye (MB and PR)

Both EFB fibers were packed at a weight ratio of 1:1 at different configurations: a layer of CA-EFB followed by a layer of PEI-EFB (CA-EFB:PEI-EFB) and vice versa (PEI-EFB:CA-EFB), and a completely mixed composition (CA/PEI-EFB). The adsorption performance of the mixed adsorbent in column was evaluated at 300 mg/L of total dye concentration, 15 mL/min of flow rate, 5 cm of bed height, 20°C, and pH 5.

3. Results and discussion

3.1. Breakthrough curve modeling

Several theoretical models have been used to describe the breakthrough behavior in continuous adsorption. The experimental data were fit to the models to obtain precise estimation of the breakthrough behavior and to evaluate the effects of different conditions on the adsorption performance of the fixed-bed columns [13]. Thomas model is based on the Langmuir adsorption/desorption model, which features non-axial dispersions and a rate driving force that follows pseudo-second order reversible reaction kinetics. The linearized equation of the Thomas model can be expressed as follows [14]:

$$\frac{C_0}{C_t} = \frac{1}{1 + \exp\left(\frac{k_{\text{Th}} q_0 m}{F} - k_{\text{Th}} C_0 t\right)} \quad (2)$$

where C_0 is the initial concentration, C_t is the concentration (mg/L) of dyes at time, t (min), k_{Th} is the Thomas rate constant (L/mg min), q_0 is the maximum solid-phase concentration (mg/g), m is the mass of the adsorbent in the column (g), V_{eff} is the volume of the effluent (L), and F is the flow rate of the effluent (L/min).

Clark model, which combines the Freundlich equation with mass transfer parameters, can be linearized as follows [15]:

$$\frac{C_0}{C_t} = \left(\frac{1}{1 + Ae^{-rt}}\right)^{1/n-1} \quad (3)$$

where n is the inverse of the slope of the Freundlich isotherm, and A and r are the Clark constants. The experimental data were fit using the non-linear estimation curves of the two models, as shown in Fig. 3, and the results are summarized in Table 1. The Thomas model provides a good fit for the experimental data of both PR and MB adsorption with an excellent correlation of r^2 ~0.99. Previous study on the adsorption of MB on CA-EFB using batch adsorption process demonstrated that the adsorption of MB on the CA-EFB is monolayer [12]. Consistent results were observed in this study using continuous fixed-bed system with acceptable values of the maximum adsorption capacity of 182.0 and 292.5 mg/g for MB and PR at 300 mg/L, respectively. Moreover, in batch adsorption studies, the maximum uptake at the same concentration of MB and PR are 130.0 and 239.4 mg/g, respectively [12].

The Clark model was used to fit the experimental data by using a parameter n to account for the difference between batch and fixed-bed adsorption [16]. As it can be observed in Table 1, the Clark model is more fit to the adsorption of PR on the PEI-EFB. At higher effluent flow rates, the value of n is nearly equivalent

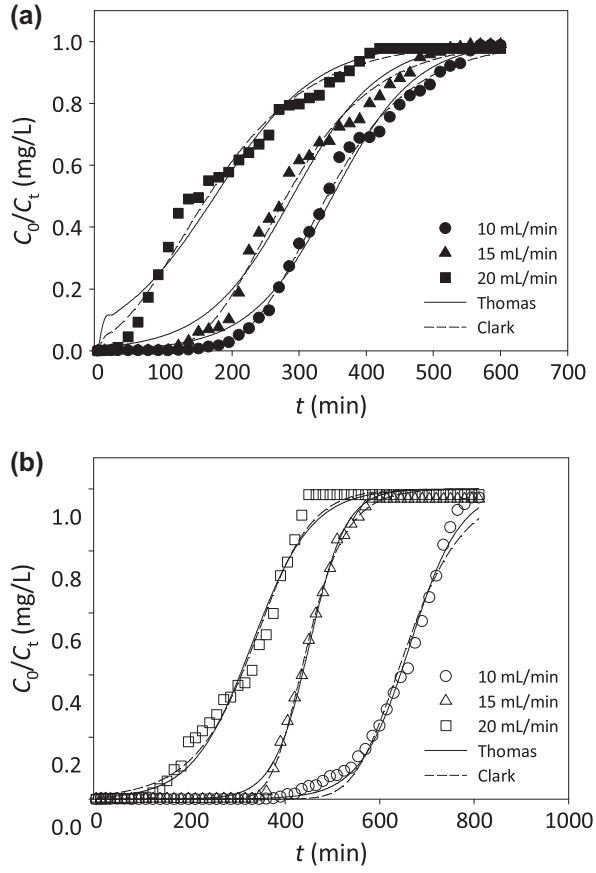

Fig. 3. Non-linearized estimation fits obtained using Thomas and Clark models at different flow rates: (a) MB with a fixed-bed CA-EFB and (b) PR with PEI-EFB (adsorbate dose: 300 mg/L; bed height: 5 cm; temperature: 20 °C; and flow rate: 10–20 mL/min).

to that of batch adsorption, suggesting that heterogeneous adsorption can occur at higher flow rates [12]. Nevertheless, the n values for both systems may slightly differ due to the different experimental setup and adsorption variables. In contrast, at slower flow rates, the adsorbate molecules become homogeneously distributed on the surface of adsorbent. Although the correlations for the Thomas and Clark models were both favorable, the adsorption of MB and PR was more accurately described by the Thomas model. It has been reported that the dynamic adsorption is a complicated process; therefore, it is almost impossible to describe its mechanism. Moreover, as compared to the batch adsorption system, dynamic adsorption has more variables which could influence the adsorption process [13].

Fig. 4(a) demonstrates that the flow rate of the effluent has a significant effect on the breakthrough for the adsorption of both MB and PR. Reducing the flow rates of the effluent leads to an increase in the contact time between the adsorbate and the packed adsorbent. The adsorption at this stage is very rapid due to the availability of active sites and a decrease in the flow rates resulting from an improvement in the distribution of the adsorbate throughout the porous fibers [17]. Furthermore, an increase in the flow rates leads to the unsaturation of the packed adsorbent and resulted in lower adsorption capacity and shorter breakthrough time.

The concentration of MB and PR also has an effect on the breakthrough adsorption curves, as shown in Fig. 4(b). The initial concentration provides a driving force to overcome mass transfer resistance between the aqueous and the solid phase. The lower initial concentration of MB and PR results in a longer breakthrough time, as can be seen that the higher the dye concentration, the steeper the breakthrough curve. Moreover, a lower concentration of dyes facilitates interactions between the unoccupied surface sites, which results in a higher adsorption yield. Previous study has demonstrated that the concentrations of dyes affect the saturation rate and the breakthrough time [18].

High temperature has been known to enhance the diffusion rate of the adsorbate molecules across the external boundary layer into the internal pores of the adsorbent due to the reduced viscosity of the solution [19]. The increase in the circulated temperature through the water jacket of the column enhanced the adsorption capacity of the column, as indicated by the longer breakthrough times in Fig. 4(c). For MB adsorption, the q_0 value was determined to be 450.4 mg/g, whereas for PR adsorption, it was 555.4 mg/g. The fixed-bed CA-EFB and PEI-EFB column exhibited a much higher adsorption capacity than previously reported in batch adsorption studies due to the increased saturation of adsorbate molecules in the packed column, which forces additional molecules inside the pore structure of the fibers.

3.2. Bed depth service time (BDST) model

Variation in the bed height influences the contact time between the adsorbate and the adsorption sites of the adsorbent. The breakthrough curves in Fig. 4(c) show that the increase of bed height for MB and PR adsorption increased the service time of the fixed-bed adsorbent. The increase in the contact time has reduced the adsorption reaction rate, leading to a higher adsorption capacity of dyes.

The BDST model was fit using experimental data to predict the adsorption performance of the fixed-bed, in response, and to evaluate any changes in the

Table 1
Calculated model constants for the adsorption of MB and PR using CA-EFB and PEI-EFB

				Thomas			Clark			
F (L min^{-1})	Z (cm)	C_0 (mg L^{-1})	T (°C)	k_{Th} (L mg^{-1} min^{-1})	q_0 (mg g^{-1})	r^2	A	r	n	r^2
MB adsorption										
0.01	5	300	20	0.5288×10^{-4}	198.8	0.999	79.35	0.014	1.62	0.998
0.015	5	300	20	0.5281×10^{-4}	182.0	0.993	0.170	0.012	1.01	0.999
0.02	5	300	20	0.4523×10^{-4}	145.3	0.999	0.020	0.010	1.01	0.986
0.015	3	300	20	0.4826×10^{-4}	165.4	0.997	8.840	0.012	2.06	0.998
0.015	7	300	20	0.3509×10^{-4}	195.0	0.999	35.88	0.010	1.87	0.999
0.015	5	200	20	0.6839×10^{-4}	171.3	0.999	82.11	0.013	1.62	0.998
0.015	5	400	20	0.3365×10^{-4}	199.7	0.994	35.88	0.010	1.87	0.961
0.015	5	200	40	0.4194×10^{-4}	203.4	0.992	0.260	0.010	1.01	0.999
0.015	5	200	60	0.3649×10^{-4}	450.4	0.999	200.0	0.009	1.48	0.997
PR adsorption										
0.01	5	300	20	0.5796×10^{-4}	309.8	0.999	564.1	0.013	1.14	0.999
0.015	5	300	20	0.8596×10^{-4}	292.5	0.999	447.6	0.019	1.14	0.999
0.02	5	300	20	0.4774×10^{-4}	281.7	0.999	320.5	0.019	2.29	0.999
0.015	3	300	20	0.7077×10^{-4}	268.3	0.999	854.7	0.020	1.55	0.999
0.015	7	300	20	0.5727×10^{-4}	350.2	0.999	338.3	0.013	1.03	0.997
0.015	5	200	20	0.4821×10^{-4}	276.0	0.999	330.4	0.009	1.63	0.999
0.015	5	400	20	0.3887×10^{-4}	308.7	0.998	87.58	0.014	1.76	0.999
0.015	5	200	40	0.4473×10^{-4}	435.0	0.999	824.6	0.014	2.28	0.999
0.015	5	200	60	0.3528×10^{-4}	555.4	0.999	234.5	0.007	1.94	0.999

column adsorbent behavior [18]. This design required the physical measurement of the fixed-bed capacity at various breakthrough values. The BDST model can be expressed by the following equation [20]:

$$t = \frac{N_0 Z}{C_0 v} - \frac{1}{k_B C_0} \ln\left(\frac{C_0}{C_t} - 1\right) \quad (4)$$

where k_B is the adsorption rate constant (L mg^{-1} min^{-1}), N_0 is the adsorption capacity (mg L^{-1}), Z is the bed height (cm), and v is the linear velocity (cm min^{-1}). The bed height (Z) was plotted as a function of time (t). The service times for 10, 20, 40, and 60% of C_t/C_0 values were selected as the points shown in Fig. 5, and the calculated values of k_B and N_0 are summarized in Table 2. Whereas the linearized MB adsorption model provided a good fit, the PR data revealed less correlation at a higher bed height, and the service times for the bed were much longer than typical for a lower bed height. The values of k_B decreased with increasing bed height, requiring a longer amount of time for a breakthrough to occur. The lower rate transfer from the adsorbate effluent to the fixed-bed column allowed the adsorbent molecules to diffuse deeper into the porous sites of the adsorbent [21]. Furthermore, the negative values calculated for $C_t/C_0 = 0.6$ are considered the limitation of the BDST model, which could only be fit by the initial part of the breakthrough curve [16].

3.3. Regeneration studies

Several adsorption/desorption cycles were performed to evaluate the regeneration performances of the CA-EFB and PEI-EFB. Fig. 6(a) shows slight reduction in the MB adsorption on CA-EFB after five cycles of adsorption/desorption processes, which is consistent with the batch adsorption study [12]. Approximately 19.1% of reduction in the adsorption capacity of the CA-EFB was calculated using Thomas model after five regeneration cycles. PEI-EFB experienced a greater reduction in the adsorption performance towards PR, as can be observed in Fig. 6(b). The severe reduction after the first adsorption/desorption cycle can be attributed to leaching of uncross-linked PEI fraction during desorption using HCl. The adsorption performance of the PEI-EFB decreased about 26.6% after five regeneration cycles.

3.4. Adsorption of mixed dyes

The anionically and cationically treated EFB fibers were used for the simultaneous removal of both MB

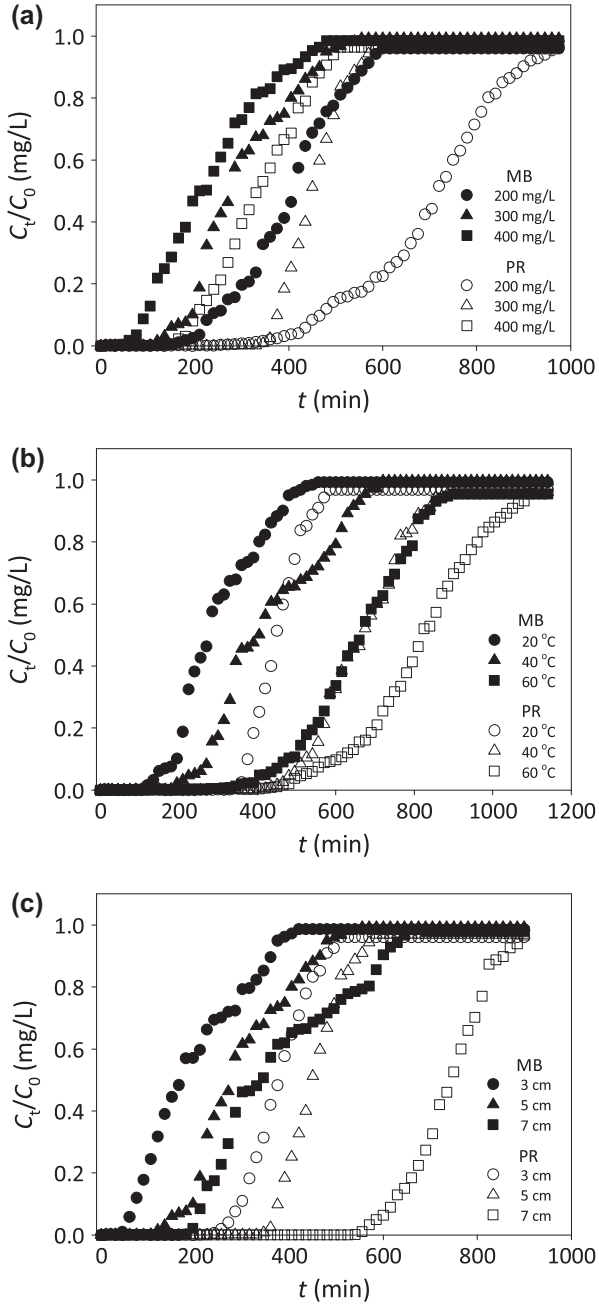

Fig. 4. Adsorption of MB and PR using a fixed-bed CA-EFB and PEI-EFB column, respectively, with different controlled parameters: (a) different initial influent concentrations, (b) different column temperatures, and (c) different column bed heights (adsorbate dose: 200–400 mg/L; bed height: 5–9 cm; temperature: 20–60˚C; and flow rate: 15 mL/min).

and PR. Fig. 7 shows the removal of MB and PR using columns packed with CA-EFB and PEI-EFB fibers with different configurations. Fig. 7(a) and (b) show the

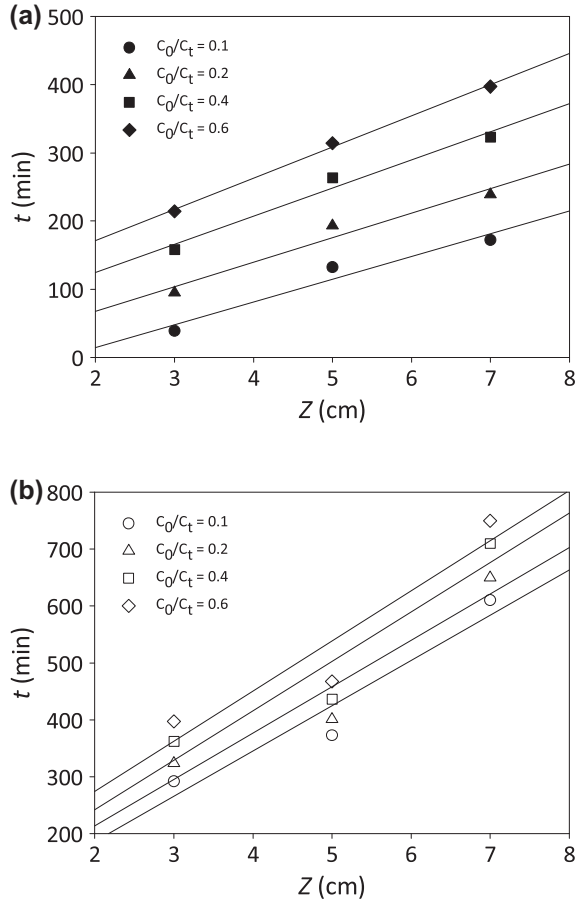

Fig. 5. Linearized plots of BDST model: (a) adsorption of MB by a fixed-bed CA-EFB and (b) adsorption of PR by a fixed-bed PEI-EFB (adsorbate dose: 300 mg/L; bed height: 5–9 cm; temperature: 20–60˚C; and flow rate: 15 mL/min).

Table 2
Experimental service time values determined using different percentages of breakthrough points according to the BDST model

C_t/C_0	k_B (L mg^{-1} min^{-1})	N_0 (mg L^{-1})	r^2
MB adsorption			
0.1	36.42	49.87	0.950
0.2	18.84	53.79	0.958
0.4	1.92	61.67	0.975
0.6	−1.36	68.23	0.997
PR adsorption			
0.1	22.09	118.76	0.925
0.2	7.16	121.88	0.915
0.4	0.89	129.84	0.901
0.6	−1.91	131.64	0.892

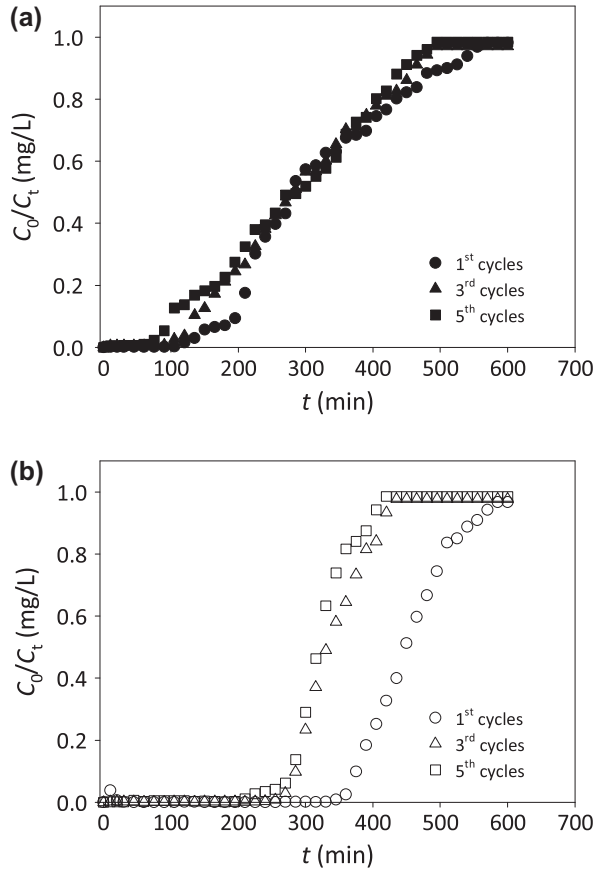

Fig. 6. Regeneration of CA-EFB and PEI-EFB for five adsorption/desorption cycles: (a) MB in a fixed-bed CA-EFB and (b) PR in a fixed PEI-EFB (total adsorbate dose: 300 mg/L; total bed height: 5 cm; temperature: 20˚C; and flow rate: 15 mL/min).

removal of MB and PR using CA-EFB:PEI-EFB and PEI-EFB:CA-EFB, respectively. Both systems exhibit almost similar removal performance as the single solute system. Nonetheless, for the column packed with mixed CA-EFB:PEI-EFB, the removal of MB is completely affected (Fig. 7(c)), as compared to the single solute system (Fig. 3(a)). This may be attributed to the interference by the highly branched and positive charged PEI on the adsorption of MB on CA-EFB. However, for the removal of PR, the performance was slightly reduced and the curve is less steep than that of the single solute system (Fig. 3(b)). The ability of the PEI-EFB in adsorbing PR, even in the presence of CA-EFB, can be due to much higher surface charge, in which the surface charge (in mV) of the PEI-EFB is two times of the CA-EFB [12].

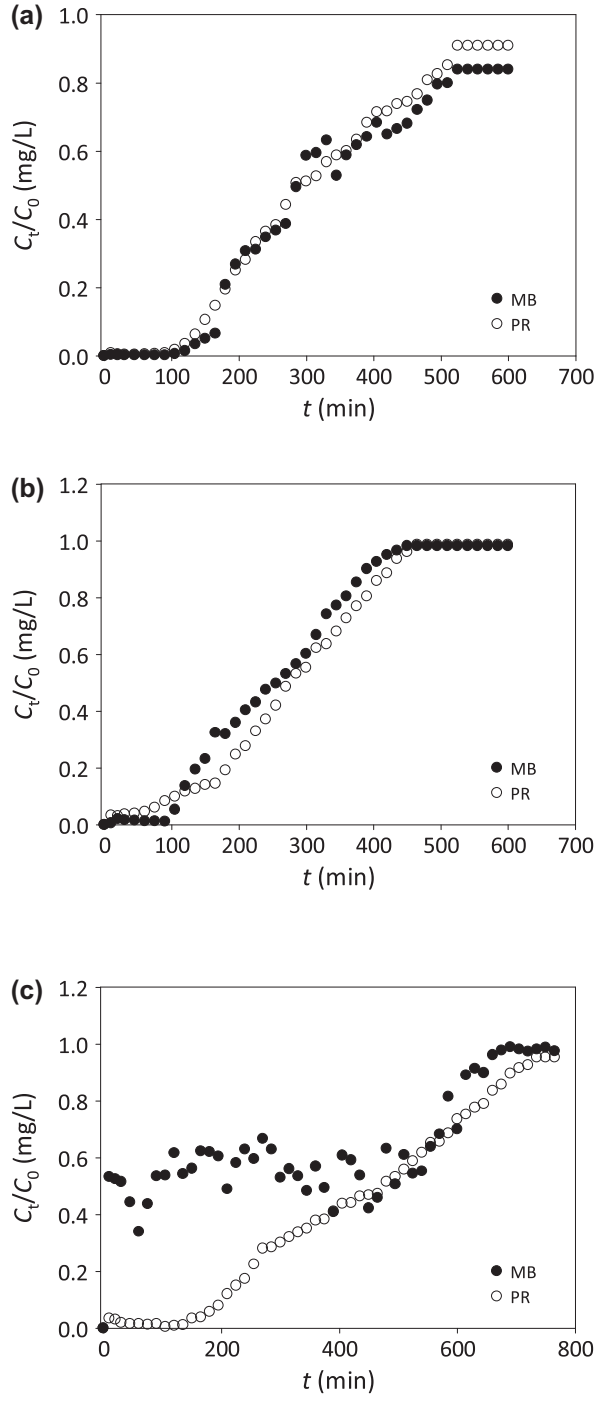

Fig. 7. Adsorption of mixed dyes (MB and PR) using a fixed-bed column with different adsorbent configurations: (a) CA-EFB:PEI-EFB, (b) PEI-EFB:CA-EFB, and (c) mixed CA/PEI-EFB fibers (total adsorbate dose: 300 mg/L; total bed height: 5 cm; temperature: 20˚C; pH: 5; and flow rate: 15 mL/min).

4. Conclusions

Cationically and anionically modified EFB fibers were used to continuously remove MB and PR in single- and multi-solute systems. The experimental data of the single-solute system could be fit by the Thomas model, suggesting the monolayer adsorption behavior of both adsorptions. The adsorption performance of both CA-EFB and PEI-EFB toward MB and PR, respectively, is significantly influenced by the adsorbate dose, bed height, column temperature, and flow rate. The column could be regenerated up to five times with slight reduction of adsorption performance. Simultaneous removal of MB and PR using column packed with CA-EFB and PEI-EFB is significantly influenced by the configuration of both adsorbents, due to the interference of surface charges of the adsorbents.

Acknowledgments

The authors acknowledge the financial support of the Universiti Kebangsaan Malaysia via the UKM-GGPM-NBT-085-2010 and DIP-2012-34 research grants.

References

[1] E. Forgacs, T. Cserháti, G. Oros, Removal of synthetic dyes from wastewaters: A review, Environ. Int. 30 (2004) 953–971.
[2] M.A.M. Salleh, D.K. Mahmoud, W.A.W.A. Karim, A. Idris, Cationic and anionic dye adsorption by agricultural solid wastes: A comprehensive review, Desalination 280 (2011) 1–13.
[3] M. Rafatullah, O. Sulaiman, R. Hashim, A. Ahmad, Adsorption of methylene blue on low-cost adsorbents: A review, J. Hazard. Mater. 177 (2010) 70–80.
[4] Z. Zhang, I.M. O'Hara, G.A. Kent, W.O.S. Doherty, Comparative study on adsorption of two cationic dyes by milled sugarcane bagasse, Ind. Crops Prod. 42 (2013) 41–49.
[5] M.J. Iqbal, M.N. Ashiq, Adsorption of dyes from aqueous solutions on activated charcoal, J. Hazard. Mater. 139 (2007) 57–66.
[6] L. Remenárová, M. Pipíška, M. Horník, M. Rozložník, J. Augustín, J. Lesný, Biosorption of cadmium and zinc by activated sludge from single and binary solutions: Mechanism, equilibrium and experimental design study, J. Taiwan Inst. Chem. Eng. 43 (2012) 433–443.
[7] V.K. Gupta, Suhas, Application of low-cost adsorbents for dye removal—A review, J. Environ. Manage. 90 (2009) 2313–2342.
[8] W.S. Wan Ngah, M.A.K.M. Hanafiah, Removal of heavy metal ions from wastewater by chemically modified plant wastes as adsorbents: A review, Bioresour. Technol. 99 (2008) 3935–3948.
[9] R. Othman, R. Ameer, Environmental disclosures of palm oil plantation companies in Malaysia: A tool for stakeholder engagement, Corp. Soc. Responsib. Environ. Manage. 17 (2010) 52–62.
[10] W.P.Q. Ng, H.L. Lam, F.Y. Ng, M. Kamal, J.H.E. Lim, Waste-to-wealth: Green potential from palm biomass in Malaysia, J. Clean. Prod. 34 (2012) 57–65.
[11] M.A.A. Mohammed, A. Salmiaton, W.A.K.G. Wan Azlina, M.S. Mohamad Amran, Gasification of oil palm empty fruit bunches: A characterization and kinetic study, Bioresour. Technol. 110 (2012) 628–636.
[12] M.S. Sajab, C.H. Chia, S. Zakaria, P.S. Khiew, Cationic and anionic modifications of oil palm empty fruit bunch fibers for the removal of dyes from aqueous solutions, Bioresour. Technol. 128 (2013) 571–577.
[13] Z. Xu, J.G. Cai, B.C. Pan, Mathematically modeling fixed-bed adsorption in aqueous systems, J. Zhejiang Univ. Sci., A 14 (2013) 155–176.
[14] H.C. Thomas, Heterogeneous ion exchange in a flowing system, J. Am. Chem. Soc. 66 (1944) 1664–1666.
[15] R.M. Clark, Modeling TOC removal by GAC: The general logistic function, J. Am. Water Works Assoc. 79 (1987) 33–131.
[16] W. Zhang, L. Dong, H. Yan, H. Li, Z. Jiang, X. Kan, H. Yang, A. Li, R. Cheng, Removal of methylene blue from aqueous solutions by straw based adsorbent in a fixed-bed column, Chem. Eng. J. 173 (2011) 429–436.
[17] E. Malkoc, Y. Nuhoglu, Removal of Ni(II) ions from aqueous solutions using waste of tea factory: Adsorption on a fixed-bed column, J. Hazard. Mater. 135 (2006) 328–336.
[18] R. Han, Y. Wang, W. Yu, W. Zou, J. Shi, H. Liu, Biosorption of methylene blue from aqueous solution by rice husk in a fixed-bed column, J. Hazard. Mater. 141 (2007) 713–718.
[19] M. Doğan, H. Abak, M. Alkan, Adsorption of methylene blue onto hazelnut shell: Kinetics, mechanism and activation parameters, J. Hazard. Mater. 164 (2009) 172–181.
[20] R.A. Hutchins, New methods simplifies design of activated carbon system, Chem. Eng. 80 (1973) 133–138.
[21] M. Tamez Uddin, M. Rukanuzzaman, M. Maksudur Rahman Khan, M. Akhtarul Islam, Adsorption of methylene blue from aqueous solution by jackfruit (*Artocarpus heteropyllus*) leaf powder: A fixed-bed column study, J. Environ. Manage. 90 (2009) 3443–3450.